Journal of Thermal Analysis and Calorimetry, Vol. 70 (2002) 897–909

TG-MS AND TG-FTIR APPLIED FOR AN UNAMBIGUOUS THERMAL ANALYSIS OF INTUMESCENT COATINGS

R. Kunze, B. Schartel, M. Bartholmai, D. Neubert and R. Schriever*

Federal Institute for Materials Research and Testing, Unter den Eichen 87, 12205 Berlin, Germany

(Received February 6, 2002; in resived form April 12, 2002)

Abstract

Thermogravimetry (TG), thermogravimetry coupled with mass spectroscopy (TG-MS) and thermogravimetry coupled with Fourier transform infrared spectroscopy (TG-FTIR) were used to characterise the thermo-oxidative behaviour of two intumescent coating materials. The temperature dependence, the corresponding volatile products and the amount of residue of the different processes were determined. Using both TG-MS and TG-FTIR results in an unambiguous interpretation of the volatile products. Characteristics such as the influence of endothermic reactions, the release of non-flammable gases, the dehydrogenation enhancing the char formation and the stability of the cellular char were discussed in detail. It was demonstrated, that TG, TG-MS and TG-FTIR are powerful methods to investigate mechanisms in intumescent coatings and that they are suitable methods in respect to quality assurance and unambiguous identification of such materials.

Keywords: intumescent coating materials, TG, TG-FTIR, TG-MS

Introduction

Intense fire affects even incombustible materials such as steel which can weaken loosing its mechanical properties. A further aspect to consider is the materials expansion under thermal loads which enhances the failure of structures. Therefore an intense fire can, and often does, result in extensive damage to building structures. The main risks are not only the destruction of the building, but a premature collapse while fire fighting teams are in the building or before the building is evacuated at all. Consequently, many construction techniques have been developed to enhance the fire resistance of the building structures and materials in an attempt to extend the stability in case of fire. Common methods applied to steel structures include different kinds of lining materials and other insulations. Such passive fire protection methods are widely used and have well proven performance; however thin film intumescent coatings are an increasingly popular and a very cost efficient method of passive fire protection. They protect materials and structures from the

* Author for correspondence: E-mail: bernhard.schartel@bam.de

1418–2874/2002/ $ 5.00
Akadémiai Kiadó, Budapest

threat of fire by forming highly effective heat barrier layers in the presence of high heat [1–3]. They can be applied easily to a variety of materials such as steel, wood, sheet rock, etc. Furthermore, a wide range of flame retardant coatings facilitates a reduction in construction material while at the same time maintaining decorative themes and ensuring sufficient fire protection.

In polymeric intumescent coatings endothermic chemical reactions are exploited to absorb heat and to produce bubbles causing the material to swell. A carbonaceous or silicate layer of a multicellular structure is formed with simultaneous release of non-flammable gases [4–7]. Originally thin, e.g. around 0.3–1.5 mm, intumescent coatings increase their thickness typically by 50–200 times when exposed to high temperatures. The blown up layer acts as an efficient heat barrier reducing the heat flux to the structure significantly. Intumescent coating materials have a complex property combination in order to fulfill all the requirements on the formation of the foam as well as on the foam properties such as low heat conductivity, high thermal stability, but also a good adhesion to the protected material. Commercially available systems consist of mixtures of distinct components such as binding agents, carbonising substances, non-flammable gas producing agents, dehydrating compounds and esterification catalysts. A large number of different chemical compounds are considered for each of these specific functions. Furthermore the timing of the chemical processes is crucial while the material is heated. The challenge in this field consists of both, finding the right combination of ingredients and optimising the quantity of them.

It is the aim of this contribution to demonstrate that thermogravimetry coupled with mass spectroscopy (TG-MS) and thermogravimetry coupled with Fourier transform infrared spectroscopy (TG-FTIR) are powerful tools to characterise the temperature dependence of the different processes as well as the volatile products and the amount of residue. Especially, using both methods promises an unambiguous insight. The results deliver a better understanding of the mechanisms and therefore enhance materials optimisation and development.

Experimental

Investigated materials

Two commercial products, System A, a water based intumescent coating, and System B, solvent containing intumescent coating, were investigated. The materials are used for intumescent coatings to increase the fire resistance of steel structures in buildings. In both materials polyacrylates act as binding agents, polyhydric alcohols as carbonising substances, melamine as a foam producing compound and ammonium polyphosphate as a dehydrating agent. Titanium dioxide is used in both materials as filler. Titanium dioxid is known to show a synergistic behaviour to the flame retardant efficiency of intumescent char forming systems [8].

Thermal analysis under air

Since the materials are non-flammable, no oxygen consuming flame zone just above the materials surface is expected in the case of fire. Therefore, all TG investigations were performed under air taking into account that the intumescent coatings act exposed to high temperature and air.

TG coupled with mass spectroscopy (TG-MS)

The TG-MS set-up consisted of a TG/DTA 220 (Seiko) coupled with a QMG 421 C quadrupole mass spectrometer (Balzer). The ambient pressure was reduced to high vacuum with a quartz capillary system enabling the online coupling of both methods [9]. The quartz capillary line was heated to a temperature of 473 K in order to restrict detection delays caused by condensation effects. The investigations were performed in the temperature range of 303 K–1173 K under air at a flow rate of 200 mL min^{-1}. A heating rate of 10 K min^{-1} was applied. The sample mass was around 5 mg. The characteristic fragments were determined and were monitored *vs.* the temperature in the multiple ion detection mode.

TG coupled with Fourier transform infrared spectroscopy (TG-FTIR)

The TG-FTIR set-up consisted of A TGA/SDTA 851 (Mettler/Toledo) coupled with a FTIR-Spectrometer Nexus 470 (Nicolet). The measurements were performed in the temperature range between 293 and 1173 K with a heating rate of 10 K min^{-1} and an air flow rate of 30 mL min^{-1}. The mass of the samples was 10.5 to 12.5 mg. The coupling capillary system was heated to 473 K and the gas sample cell of the FTIR spectrometer to 483 K. The sample cell was cleaned with a 1373 K hot oxygen stream after every measurement to minimize the influence of condensations.

Results

Both materials are characterized by a multistep decomposition in terms of mass loss. Figures 1 and 2 show the TG, DTG and DTA for the two materials. Seven (System A) and six steps (System B) can be separated. They are named step I up to step VII or VI, respectively, according to the increasing temperature of their occurrence. The corresponding TG and DTG data are summarized in Table 1. It records the averaged results of the TG experiments which were performed with two different instruments and sample masses. The results correspond well with each other, with exception to the temperature range of process V which is shifted due to the fact that the used sample differs in mass and was transformed into isolating char during step I to IV.

In first approximation, the characteristics are qualitatively similar for both samples, especially in terms of the first five steps showing rough correspondence in their mass losses and similar temperature ranges. Furthermore, the mass loss of step VI of System B corresponds to the sum of the mass losses of step VI and step VII of System A. All steps show some form of an overlap with the preceding and the following step,

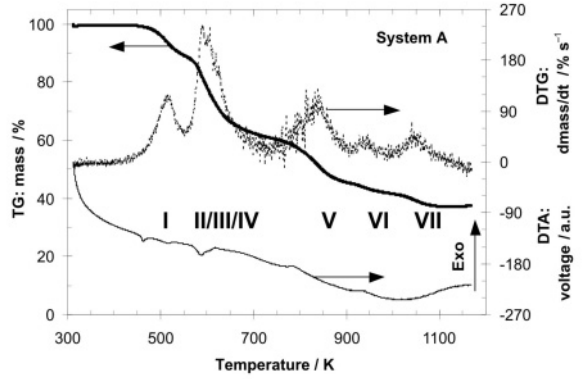

Fig. 1 TG, DTG and DTA results for System A

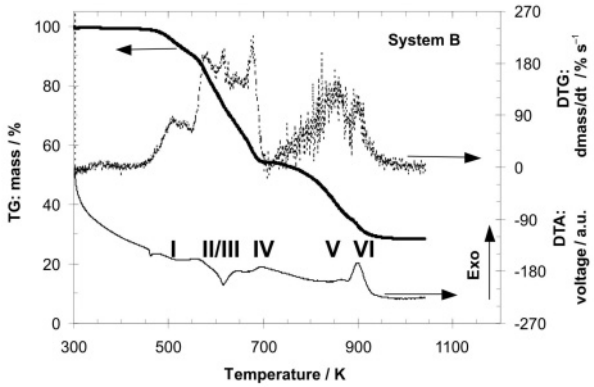

Fig. 2 TG, DTG and DTA results for System B

especially step II, III and IV for the sample System A, where step III and IV is only indicated by a shoulder in the DTG data. Both samples exhibit large amounts of residue close to a third of the starting mass even beyond 1150 K and large residues after the first decomposition steps I–IV at temperatures up to 750 K, with even less than a drop in 50% mass. Therefore the TG data clearly indicate char forming processes beyond the content of thermal stable inorganic fillers. Comparing the two materials in detail, System A produces the larger amount of residue after the first decomposition steps as well as for very high temperatures.

Figures 3–6 illustrate the TG-MS results for System A and System B. The ion currents for different fragments are illustrated together with the corresponding TG data. The distinct decomposition steps result in different characteristic ions. Key ions or typical series of fragments indicate the kind of pyrolysis gases released. Hence, the distinct molecular origins of the different processes can be illuminated.

Figure 7 shows an overview of the TG-FTIR investigation for System B. Spectra at distinct temperatures were used to evaluate the composition of the pyrolysis gases.

Table 1 TG data. The values are averaged values of the different experiments which are performed with different instruments and different masses

	System A				System B			
Step	Mass loss /% ± 0.5% K^{-1}	DTG *T*(peak)/ K±1	DTG peak/ % K^{-1}	Residue/% ±0.5	Mass loss/% ±1	DTG peak *T*(peak)/ K±1	DTG peak/ % K^{-1}	Residue/% ±0.5
I	10.5	513.1	19.7	89.3	9.1	510.3	14.6	90.9
II	28.7	588.9	38.5	60.5	14.0	577.0	32.9	76.7
III		603.8			7.5	615.8	29.5	69.2
IV		(~ 620)*			15.0	674.6	32.2	54.2
V	15.5	837/870#	16.3	45.1	18.3	851/862#	21.2	35.9
VI	3.1	943.4	6.4	42.0	7.8	901.45	17.1	28.1
VII	4.4	1033.3	6.3	37.7				

*A corresponding increased mass loss is only marked by a shoulder

The process V is clearly shifted for the measurements with higher and swelled masses, so that no average value was calculated

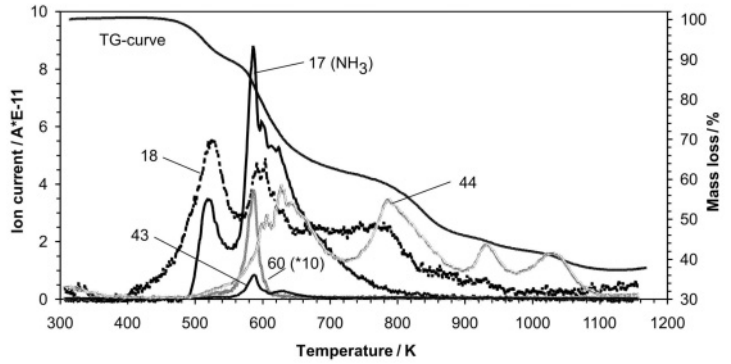

Fig. 3 TG-MS-curves for System A with a sensitivity of 10^{-11} A. The signal for NH_3 (m=17 u) is corrected by subtraction of the OH^- contribution

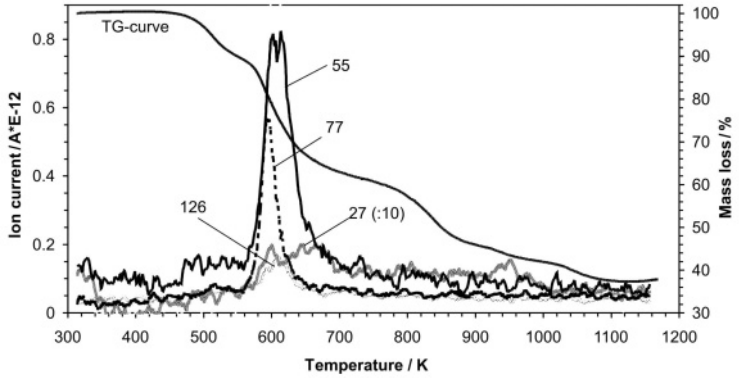

Fig. 4 TG-MS-curves for System A with a sensitivity of 10^{-12} A

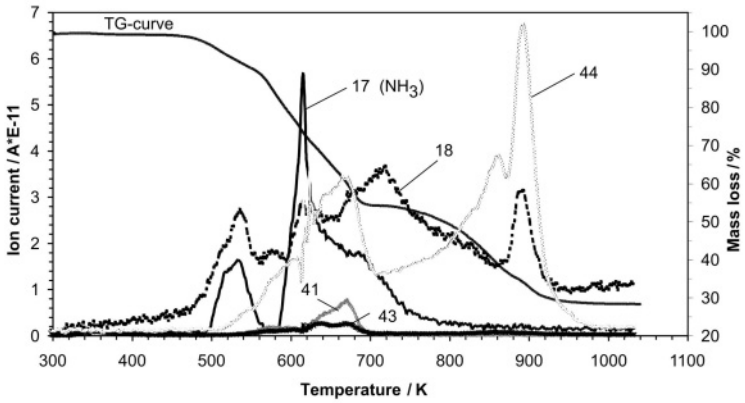

Fig. 5 TG-MS-curves for System B with a sensitivity of 10^{-11} A. The signal for NH_3 (m=17 u) is corrected by subtraction of the OH^- contribution

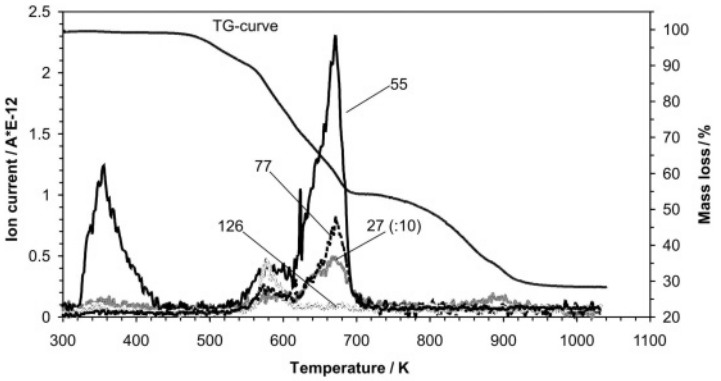

Fig. 6 TG-MS-curves for System B with a sensitivity of 10^{-12} A

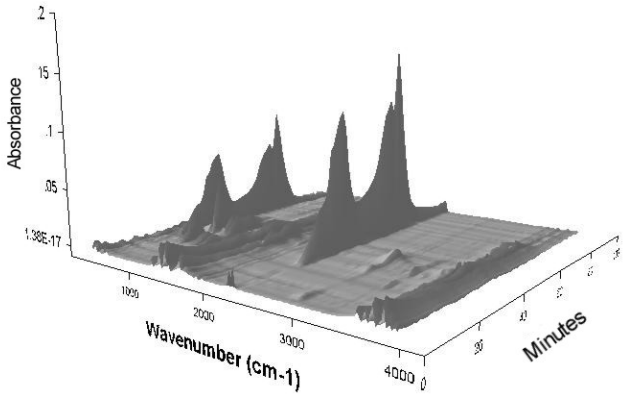

Fig. 7 FTIR spectras of the pyrolysis gases during the TG experiment (heating rate: 10 K min^{-1})

Certain extinctions being characteristic for specific functional groups of the evolved gases provide the so-called chemigrams *vs.* the experimental time or temperature, respectively. Such chemigrams provide information on the release rate of the pyrolysis gases during the TG experiment similar to the ion currents of TG-MS investigation. Details of the TG-FTIR-measurements (chemigrams) are plotted in Figs 8 and 9 *vs.* the temperature. The chemigrams and the ion current data correspond well with each other, proving an unambiguous description of the pyrolyse gases. Furthermore, step I, II, III and IV correspond to the DTG data so that a detailed and complete picture of these decomposition steps emerges. Comparing the two independent methods used to investigate the pyrolysis gases, an unambiguous identification of the gases was possible. H_2O, NH_3, CO_2 and hydrocarbons were found in both materials to be the main pyrolysis gases. For System A in addition to these main products ethanoic acid (m/e= 60 u) was detected by TG-MS and TG-FTIR. With the more sensitive mass spectroscopy a signal for m/e=126 u can be found for both materials, which corresponds to the molecular mass of melamine. A mass signal close to the resolution of the equipment in-

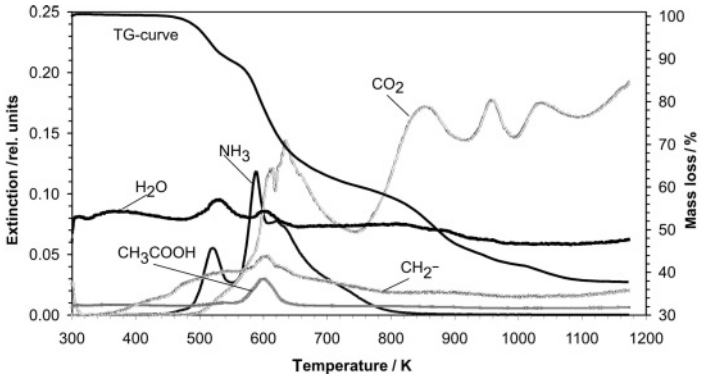

Fig. 8 Chemigrams for selected pyrolysis gases of System A

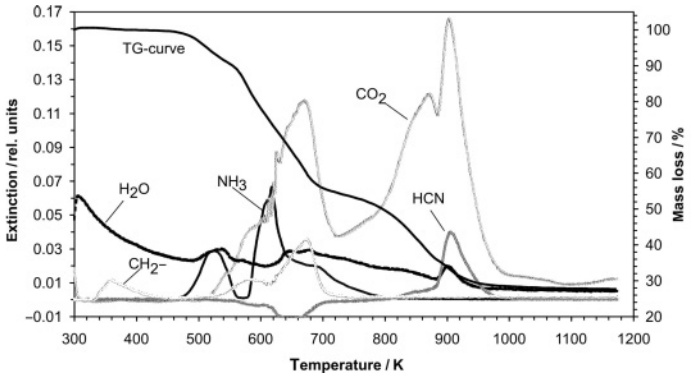

Fig. 9 Chemigrams for selected pyrolysis gases of System B

dicates phosphorus pentoxide in System B. Furthermore the comparison of the chemigrams for HCN and the ion-current curve for *m*/*e*=27 u shows that a release of HCN takes place above 900 K. The ion-current curve for *m*/*e*=27 u in the temperature region of 620–820 K is connected with C_2H_3 because the identical run with the curves of the C_nH_m-pyrolyse products.

In Table 2 the characteristic pyrolysis gases are shown for the distinct decomposition steps. For the decomposition steps at temperatures above 750 K in the case of System A significant deviations were found between the rates of pyrolysis gas release detected with TG-MS and TG-FTIR and the mass loss rate. CO_2 release precedes the mass loss if the temperature increases. It is most likely that the mass loss of this high temperature decomposition is controlled not only by the release of the detected small products CO_2 and H_2O but also by products which could not be detected possibly because they were not able to pass the connection between the TG and the gas analysing equipment due to their large size or their unfavourable condensation behaviour.

Table 2 Pyrolysis gas release

Decomposition step	System A	System B
I	H_2O, NH_3	H_2O, NH_3
II	H_2O, NH_3, ethanoic acid, C_nH_m	H_2O, C_nH_m, melamin
III	NH_3, H_2O, C_nH_m, melamin	H_2O, NH_3, C_nH_m
IV	NH_3, H_2O, CO_2, C_nH_m	H_2O, NH_3, CO_2, C_nH_m, P_2O_5
V	CO_2, H_2O	CO_2, H_2O
VI	CO_2, (HCN)	CO_2, H_2O, HCN
VII	CO_2	

Discussion

Comparison between TG, TG-MS and TG-FTIR

In comparison to TG illustrating the thermal decomposition in terms of the mass loss, TG-FTIR and TG-MS extend the thermal analysis by additional monitoring and identification of the pyrolysis gases (Figs 3–9). It is obvious that such a characterization of the decomposition profits greatly by this additional information and delivers a detailed insight into the decomposition processes. However, the interpretation of the FTIR is often difficult since a superposition of the various signals from the different gases can lead to complex spectra. In the case of TG-MS the ionisation of the decomposition fragments can result in ambiguous mass signals. By using both methods unambiguous interpretations of the data were obtained without using further assumptions on the material or the active decomposition pathway.

Endothermic reactions

Intumescent coatings can protect their substrate from heat treat by two mechanisms: Firstly, a heat sink mechanism, which means that heat is absorbed by endothermic chemical reactions. Secondly, the low thermal conductivity of the coatings reduces the heat flux into the sample. The first mechanism is successfully used in fire retardant polymeric materials with a high content (40–60% load) of inorganic filler systems like $Mg(OH)_2$ or $Al(OH)_3$ [10]. The fireproofing effect of a thin coating, of course, is limited by the limited amount of fire retardant in relation to the substrate material. Furthermore, the small thickness of coating limits the thermal insulation needed for a promising effect due to the second mechanism. Therefore, a key property of thin intumescent coatings is to produce a thick insulating layer via endothermic chemical reactions.

Step I, II, III and IV are all characterized by endothermic behaviour (Figs 1 and 2). The associated processes provide heat sink mechanisms. In contrast to the performed TG experiment with a constant heating rate, in a real fire scenario a certain external heat flux will effect the material. Hence, the associated endothermic processes slow down the tem-

perature increase of the protected underlying layers and substrate. The endothermic character of the reactions and the increasing heat barrier due to the already formed intumescent char ensure that the time interval is increased for the temperature range in which an effective intumescent char can be formed.

Release of non-flammable gas

Apart from the endothermic reactions and the char formation the release of non-flammable gases is essential for intumescent polymeric coatings. The release of H_2O and NH_3 is associated with the decomposition step I, II, III and IV (Figs 3, 5, 8, 9, Table 2). CO_2 is additionally released in step IV. The gases serve in two different ways. Firstly, they are necessary to form the bubbles in the multicellular structured char which creates the insulating properties. Secondly, they provide a flame blanking and heat sink if they are released. It is obvious, that the efficiency of an intumescent layer would be significantly decreased if the released gases are combustible and increase the heat flux effecting the surface. H_2O, NH_3 and CO_2 are all non-flammable and cannot result in an additional heat production by combustion. On the contrary, they are able to dilute the fuel gases in surrounding flame zones. Furthermore, they work as cooling agents in the gas phase. Especially water but also ammonia are characterised by high products of their heat of gasification (H_2O: 2.256 kJ g^{-1}; NH_3: 1.4 kJ g^{-1}) and its volume of gas per g at $T_{decomposition}$ (H_2O: 1244 mL g^{-1}; NH_3: 1318 mL g^{-1}) [11]. Hence, the production and release of NH_3 and H_2O represent key processes for sufficient intumescent coatings, whereas the production of CO_2 can be connected with extensive heat production in contrast to its fireproofing properties in the gas phase.

Dehydrogenation

Sufficient intumescent systems are not only characterised by the formation of a multicellular char but also by an effective production in terms of a large amount of such a char. The key process to enhance the char formation is the dehydrogenation. The formation of larger aromatic molecular structures is enhanced, whereas the scission and release of hydrocarbons is decreased. Both samples investigated show a sufficient dehydrogenation by the release of hydrogen in form of H_2O and NH_3 in the first steps (Figs 3, 5, 8, 9, Table 2) and the large amount of residue at temperatures even above 700 K (Figs 1 and 2, Table 1). In the case of System A the further decomposition of the residue in the step V, VI and VII with only the one main product CO_2 illuminates a nearly complete dehydrogenation in the first decomposition processes.

Thermal stability of the cellular char

The fire retardant effect of intumescent coatings is based on insulation by a heat barrier rather than an increased thermal stability. In fact, the time interval is increased before the structure reaches a critical temperature enhancing mechanical failure or a further spread of the fire, whereas the temperature limits remain unchanged. How-

ever, the thermal stability of the char limits also the lifetime of the fire retardant intumescent system and controls the temperature ranges where the system is active in terms of fire retardancy. The onset of mass loss occurred between 430 and 455 K (Figs 1 and 2, Table 1) and is associated with dehydrogenation and the release of non-flammable gases (Table 2). The multicellular char formed in the first decomposition step is assumed to be stable in its major parts up to 750–770 K before an exothermic oxidation to CO_2 and H_2O occurs. Therefore, the temperature interval between 450 and 750 K defines the temperature range for the most efficient use as fire retardant, even though a residue of around a third of the original mass is still stable even at higher temperatures.

At elevated temperatures steel loses considerable tensile strength [12, 13]. A failure becomes imminent under full design loads when 60% of the original strength remains, since the safety factor has been reduced to one. The corresponding critical temperature is 811 K for regular reinforcing steel, whereas significantly lower critical temperatures at 700 K are known for prestressing steel bars, which are made of high carbon, cold drawn steel [14]. Apart from such critical temperatures the expansion of steel marks an increasing problem for increasing temperatures in respect to the stability of a three-dimensional construction. Hence, it can be concluded that the temperature range characterised by an efficient fire retardancy of the investigated coatings is optimised to prevent premature mechanical failure of a steel construction.

Fire risks and fire hazards

As described before the systems act as efficient fire retardant covering layer on substrates in a wide temperature range up to 750 K. The non-flammable blanking gas release and the endothermic character of the first decomposition steps rules out intrinsic fire risks of the coatings. For System B the release of HCN was detected above 900 K by the high sensitive mass spectroscopy and also by the TG-FTIR-measurements. The release of HCN for System A cannot be detected unambiguously. Since the amount of HCN was too small to be detected with the FTIR equipment it could be assumed to be of minor importance. The decomposition processes above 750 K are exothermic, but the detected products are still not suitable to feed a flame.

Comparison of the materials

The main characteristics are qualitatively similar for the materials, but show significant differences in some details (Tables 1, 2 and Figs 1–9). Both materials show the three overlapping decomposition steps, step II, III and IV in the temperature range between 570 and 750 K with similar main products. However, the products release rates deviate significantly between the two samples. Most notable is the occurrence of a volatile product exclusively for each of the materials like ethanoic acid for System A and P_2O_5 for System B, respectively. Furthermore the release rate maximum for NH_3 is associated with decomposition step II for System A, and with decomposition step III for System B. Similar changes were found for melamin and some hydro-

carbons. Concerning the oxidation of the char at temperatures above 750 K decomposition process V is very similar for both materials, whereas the subsequent further decomposition is clearly different in terms of temperature range and release of H_2O.

Conclusions

TG coupled with spectroscopic gas analysis was demonstrated to be a powerful tool for the investigation of intumescent coatings. It delivers a detailed insight into the thermal behaviour of the materials characterised by mass loss, which controls the fire retardant function of these materials. The online coupling ensures not only the determination of pyrolysis gases but also the release rates during the decomposition. Using different gas analysing methods like MS and FTIR increases the unambiguous interpretation of the results.

Therefore TG, especially TG-MS and TG-FTIR are suitable methods to characterise intumesent coatings in respect to quality assurance and unambiguous identification. Especially the latter is of major importance in obtaining technical approvals for construction products and types of construction on the basis of the building regulations. TG methods show advantages in comparison to DSC measurements which are used nowadays to characterise intumescent coatings or are even laid down in technical rules for that purpose. The additional information on the volatile product is more than subsidiary data and enable a more precise characterisation. It enables a deeper understanding of the chemical processes. Hence, TG-MS and TG-FTIR are promising tools which can successfully used in materials development and optimisation.

References

1 H. L. Vandersall, J. Fire & Flammability, 2 (1971) 79.
2 M. Kay, A. F. Price and I. Lavery, J. Fire Retardant Chem., 6 (1979) 69.
3 E. Martin and T. Ward, J. Fire Retardant Chem., 8 (1981) 199.
4 M. Le Bras, G. Camino, S. Bourbigot and R. Delobel, (Eds.) Fire Retardancy of Polymers the Use of Intumescence, The Royal Society of Chemistry 1998, Special Publication 224.
5 G. Camino, Fire Retardant Polymeric Materials, in Atmospheric oxidation and antioxidants, Vol. II, Eds. G. Scott, Elsevier Amsterdam 1993, Chap. 10.
6 J. W. Lyons, The Chemistry and Uses of Fire Retardants, Wiley Interscience USA 1970.
7 G. Camino and S. Lomakin, Intumescent Materials, in Fire Retardant Materials, Ed. A. R. Horrocks and D. Price, Woodhead Publishing and CRC Press Cambridge 2001, p. 318.
8 D. Scharf, R. Nalipa, R. Heflin and T. Wusu, Fire Safety J., 19 (1992) 103.
9 R. Kunze, D. Neubert, K. Brademann-Jock and U. Erhardt, J. Therm. Anal. Cal., 53 (1998) 27.
10 W. E. Horn Jr., Inorganic Hydroxides and Hydroxycarbonates: Their Function and Use as Flame-Retardant Additives, in Fire Retardancy of Polymeric Materials, Ed. A. F. Grand and C. A. Wilkie, Marcel Dekker, New York 2000, p. 285.
11 H. Horacek and S. Pieh, Polym. Int., 49 (2000) 1106.

12 T. Z. Harmathy and W.W. Stanzak, Elevated temperature tensile and creep properties of some structural and prestressing steels, American Society for Testing and Materials, Special Technical Publication 464 on Fire Test Performance, Philadelphia, PA 1970, p. 186.
13 R. Hass, C. Meyer-Ottens and E. Richter, Stahlbau Brandschutz Handbuch, Verlag Ernst & Sohn, Berlin 1993.
14 A. E. Coté and J. L. Linville (eds.) Fire Protection Handbook, 16th Edition, Fire Safety in Building Design and Construction, National Fire Protection Association, Quincy, MA, 1986, p. 7.